Effects of Rain Drop Size Distribution Variations on Microwave Brightness Temperature Calculation

Dorothée Coppens and Ziad S. Haddad

Jet Propulsion Laboratory, California Institute of Technology, Pasadena, California 91106

e-mail : dorothee@AlbertoVO5.jpl.nasa.gov

Abstract

Current passive-microwave rain-retrieval methods are largely based on databases built off-line using cloud models : the models are used to simulate rain events, and radiative transfer calculations produce the associated brightness temperatures. The radiative transfer models depend on, among others, the distribution of hydrometeor sizes. The most popular rain drop size distribution (DSD) used in most models is Marshall and Palmer's (1948). Improvements were proposed later by, among others, Sekhon and Srivastava (1971), Willis and Tattelman (1989) and Feingold and Levin (1986). Using these DSD models, we study the dependence of forward radiative transfer calculations on the hydrometeor size distribution, and quantify the uncertainty due to DSD variability.

Keywords

Brightness temperature, Drop Size Distribution, TRMM mission.

I. Introduction

Most radiative transfer models currently used to calculate the expected microwave brightness temperatures associated with a given rain event assume that the rain drops are distributed according to the Marsall-Palmer drop size distribution (DSD) (see, e.g., [7]). This distribution is an exponential function $N(D)$ which allows one parameter, Λ, to depend on the rain rate :

$$N(D)\ dD = N_0\ e^{-\Lambda D}\ dD \quad \text{drops of diameter } D \text{ mm, per m}^3. \tag{1}$$

This representation of the DSD is simple hence easy to use in practice, and it is representative of the distribution of the drop diameters if the latter are sampled over a sufficiently long time ([6]). However, it has at least two drawbacks which can be expected to affect radiative transfer calculations significantly :

1. N_0 is assumed constant, and if one starts with a given rain rate R_0, calculates Λ and N_0, then computes the expected rain rate $R_1 = C \int v(D) D^3 N(D) dD$ (where v is the drop fall speed), one finds

that R_1 typically significantly exceeds R_0. If one does not resolve this contradiction, one's results are quite likely to be inconsistent.

2. an exponential distribution generally tends to overestimate the number of both the smallest drops [14] and the largest drops [6].

Sekhon and Srivastava proposed an exponential model in which N_0 depends on the rain rate ([11], [12]). While they find better fits for the radar reflectivity factor Z, precipitation content W and median volume diameter D_0, their model again produces a rain rate that is inconsistently quite different from the one used to specify the parameter values. Willis and Tattleman ([16]) proposed a Γ-distribution function,

$$N(D)\, dD = N_0\, D^{\mu}\, e^{-\Lambda D}\, dD \tag{2}$$

based on an improved characterization of coalescence growth and evaporation. Their parameters N_0, μ and Λ are determined by the rain rate, and, happily, do not go on to produce an inconsistently different rain rate when the latter is calculated from (2). However, since observations show that the DSD is not entirely determined only by the rain rate, it is desirable to find a parametrization for the Γ model in which the parameters have the correlations implied by the observations. Such a parametrization was derived in [5]. For completeness, we also consider a log-normal DSD model.

Armed with these five models for the DSD, we have tried to quantify the effect of variations in the drop size distribution on the calculated brightness temperatures. The main application is to the Tropical Rainfall Measurement Mission (TRMM), whose passive TRMM Microwave Imager (TMI) measures nine brightness temperatures at 10.7 (V and H polarizations), 19.3 (V and H), 22.2 (V), 37 (V and H), and 85.5 GHz (V and H). The look angle is always assumed to be 52°, and the rain is always assumed to fall on a 290K ocean surface. The various DSD models are described and compared in section II. The radiances obtained with these DSD models using Kummerow's Eddington-approximation radiative transfer model are studied in section III.

II. Comparison of the different DSD models

Marshall and Palmer's exponential distribution (1) is of course a special case of the Γ distribution (2) with $\mu = 0$. They found that the slope parameter λ which best models their data depends on the rainfall rate R and is given by $\Lambda = 4.1R^{-0.21}\ mm^{-1}$ with the R in mm/hr. N_0 is a constant, $N_0 = 8000\ m^{-3}mm^{-1}$. However, using the terminal drop fall velocity $9.65\ (1 - e^{-0.53D})\ m/sec$ for a drop of diameter D mm (see [2] – our fall velocity formula has the advantage of being always positive

for positive D, and is at worst within 4% of the measurements of Gunn and Kinzer ([3])), the re-calculated rain rate exceeds the original R by a proportion which decreases from about 20% when $R = 1$ mm/hr to 11% at 20 mm/hr and a still-significant 8% at 40 mm/hr. To make the Marshall-Palmer representation consistent without changing the value of Λ, one must modify N_0. The terminal drop velocity formula above implies that

$$N_0 = 2590 \frac{R^{0.16}}{1-(1+0.13R^{0.21})^{-4}} \; m^{-3}mm^{-1}. \tag{3}$$

is indeed consistent. We shall distinguish between the original Marshall-Palmer distribution "MP0", and the self-consistent modification "MP" as in (3).

Sekhon and Srivastava ([12]) proposed a somewhat different exponential form for the DSD. By relating various parameters such as the median volume diameter, water content, rainfall rate and radar reflectivity factor, they found a non-constant $N_0 = 7000\ R^{0.37}\ m^{-3}mm^{-1}$, and $\Lambda = 3.8\ R^{-0.14}\ mm^{-1}$. Yet in this case too, with any reasonable approximation for the drop fall velocity, one would calculate a rain rate that is about 60% larger than the original one. To make the formula consistent in this case without changin the expression for Λ, one must use $N_0 = 4400\ R^{0.37}\ m^{-3}mm^{-1}$. We shall refer to this distribution as the "SS" distribution.

Based on estimates of drop coalescence growth, Willis and Tattelman ([16]) proposed a new Γ-distribution with $N_0 = 34338.5R^{0.0245}\ m^{-3}mm^{-1}$, $\mu = 2.16$ and $\Lambda = 5.681R^{-0.153}\ mm^{-1}$. This DSD model is self-consistent and will be referred to as "WT".

Finally, Feingold and Levin ([1]) proposed a three-parameter lognormal distribution, which we shall refer to as "LOG",

$$N(D) = \frac{N_T}{\left(\sqrt{2\pi}\ log(\sigma)\ D\right)} exp\ (\frac{-log^2(D/D_g)}{(2\ log^2(\sigma))}) \tag{4}$$

with $\sigma = 1.43$ and the remaining two parameters related to the rain rate R by the expressions $D_g = 0.75\ R^{0.21}$, $N_T = 172\ R^{0.22}$.

Since knowledge of the rain rate by itself is clearly not sufficient to determine the DSD, closed-form expressions such as (2) are most useful if they can reflect the joint behavior of the parameters N_0, Λ and μ. The latter can be determined from sampled drop size distributions. Studies of the joint behavior of the DSD parameters have indeed been conducted (see e.g. [4], [5]), and reveal that one can re-express these parameters in terms of three *uncorrelated* parameters R, S'' and D'' :

$$N(D) = N_0(R, S'', D'')\ D^{\mu(R,S'',D'')}\ e^{-\Lambda(R,S'',D'')D}, \tag{5}$$

where R is the rain rate, S'' is the "normalized" relative mass-weighted deviation of the drop diameters and D'' the "normalized" mean drop diameter. By "normalized" we mean that the dependence on the rain rate has been factored out. More specifically,

$$\mu = \frac{1}{s''^2 D''^{0.33} R^{0.074}} - 4 \tag{6}$$

$$\Lambda = \frac{1}{s''^2 D''^{1.33} R^{0.23}} \tag{7}$$

$$N_0 = 55 \frac{\Lambda^{\mu+4}}{\Gamma(\mu+4)\left(1-(1+0.53/\Lambda)^{-\mu-4}\right)} R. \tag{8}$$

Based on the TOGA/COARE data, D'' has a mean of 1.13 and a standard deviation of 0.32, while the mean of S'' is 0.39 with a negligible standard deviation of 0.025. These results were corroborated by data from Darwin ([4]). It was also observed from these data sets ([5]) that while S'' varied little over all samples, D'' had a smaller mean for events with low rain rate than for those with higher rain rates : the conditional mean of D'' decreases as the rain rate increases.

To compare the various DSDs under consideration, one can start by looking for the values of the normalized mean drop diameter D'' and of the normalized relative deviation S'' which best fit each of MP, SS, WT and LOG. In fact, for a given rain rate, one can compute from (6) and (7) the exact value of the corresponding parameters for MP, SS and WT, since all three are themselves Γ-distributed, namely

	MP	SS	WT
D''	$0.976\ R^{\ 0.054}$	$1.053\ R^{\ -0.016}$	$1.08\ R^{\ -0.003}$
s''	$0.502\ R^{\ -0.046}$	$0.496\ R^{\ -0.033}$	$0.397\ R^{\ -0.036}$

TABLE I

Pointwise fits of the normalized mean diameter D'' and the relative deviation S'' for (MP), (SS), (WT) and (LOG).

Note that the WT values are remarkably close to the means determined from the data. The SS values of D'' are somewhat low, while those of S'' are rather high, an observation which is consistent with the fact, mentioned earlier, that the exponential tends to overestimate the concentration of smaller and larger drops. This trend is also evident in the MP values. Equally important to note is the fact that only MP produces a mean diameter which increases slightly with the rain rate : SS, WT and the data imply the reverse.

While this point-wise comparison cannot be carried out for the lognormal distribution, a fit can be performed over a range of rain rates : one can look for the values of D'' and S'' which best fit LOG,

	$0.5 < R < 5$ mm/hr			$5 < R < 50$ mm/hr		
	minimization criterion :			minimization criterion :		
	$N(D)$	$D^3N(D)$	$D^6N(D)$	$N(D)$	$D^3N(D)$	$D^6N(D)$
MP- S''	0.47	0.48	0.48	0.43	0.43	0.43
MP- D''	0.98	1.05	1.04	1.20	1.18	1.20
SS- S''	0.47	0.48	0.48	0.44	0.44	0.44
SS- D''	1.00	1.05	1.05	1.00	0.99	1.00
WT- S''	0.38	0.38	0.38	0.35	0.35	0.35
WT- D''	1.08	1.09	1.09	1.07	1.06	1.08
LOG- S''	0.35	0.35	0.35	0.35	0.35	0.35
LOG- D''	1.35	1.25	1.21	1.60	1.54	1.40

TABLE II

Optimal values of the normalized mead drop diameter D'' and the relative deviation S'' for (MP), (SS), (WT) and (LOG), judging the fit according to of the DSD ($N(D)$), the water volume ($D^3N(D)$) or the reflectivity ($D^6N(D)$) .

WT, SS and MP, respectively, over a given rain interval. Three different r.m.s. criteria were considered to judge the "best" fit, namely minimizing the difference in

a) the DSD $N(D)$ itself

b) the calculated liquid volume, which is proportionnal to $D^3N(D)$

c) the radar reflectivity factor Z, itself proportionnal to $D^6N(D)$.

The minimizations were performed for two rain-rate intervals, 0.5 to 5 mm/hr and 5 to 50 mm/hr. The results are summarized in table II.

Again, the WT values are quite close to the point-wise values determined above and to the means determined from the data. Also as before, the SS and MP values of S'' are rather high, consistent with the over-estimation by the exponential of the concentration of large and small drops. Most important, MP and LOG imply a mean diameter which increases with the rain rate, while SS, WT and the data imply the reverse. Note finally that the mean drop values for LOG are significantly larger than the empirical mean.

III. Effect of the DSD models on the brightness temperatures

It has already been noted that the vertical distribution of hydrometeors within a cloud has a significant impact on the resulting upwelling brightness temperatures ([13], [10]). To quantify this impact, Kummerow's Eddington-approximation forward radiative transfer model ([8]) was used to calculate the radiances produced by the DSDs described in the previous section, for simple hypothetical atmospheres as well as for simulated rain events included in the TRMM cloud-model database.

Figure 1 shows the 10.7GHz vertically-polarized and 37GHz horizontally-polarized brightness temperatures for an atmosphere with homogeneous rain extending from the surface up to 4.5 km, with the parametrized DSD (5) using different values of D''. For any given rain rate, as D'' increases, so does the 10.7GHz brightness temperature. At 37 GHz, the same is true for very low rain rates; however,

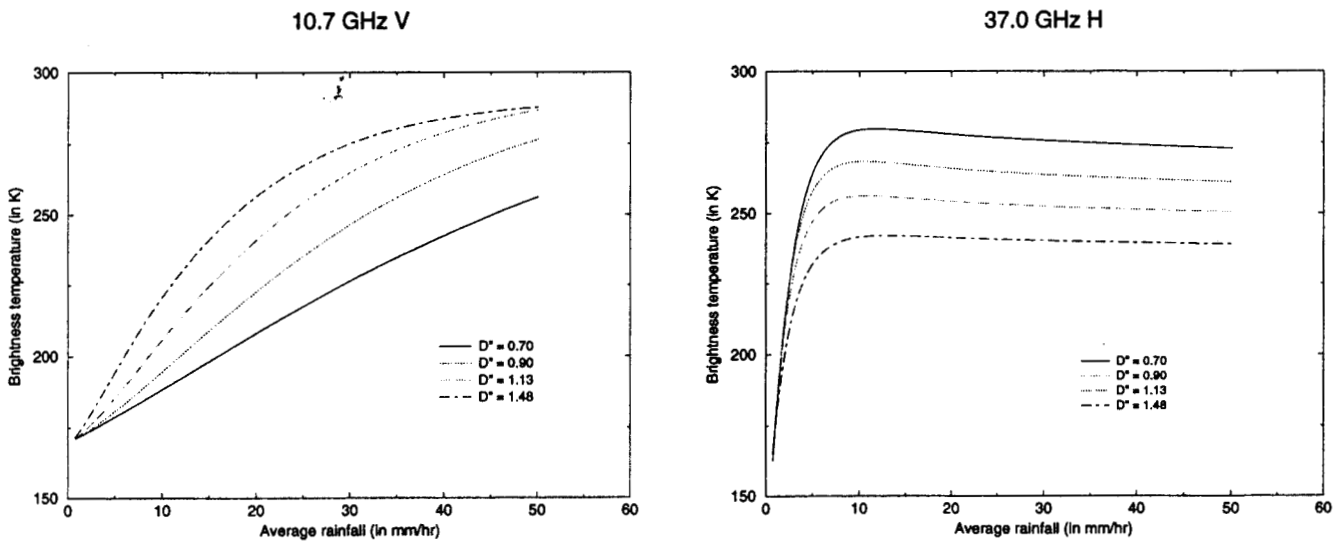

Fig. 1. *10.7GHz V-pol and 37GHz H-pol brightness temperatures for homogeneous rain with various values of D''.*

starting at about 2 mm/hr, the brightness temperature decreases as D'' increases. This is due to the fact that at lower frequencies such as 10GHz absorption is the dominant effect, while scattering starts to dominate as the frequency (and the rain rate) increase. Both effects are more significant for larger drops, hence the contrary trend at low and higher frequencies. This leads one to expect that the effect of the varying DSD should be minimized at a frequency between 10 and 37 GHz : indeed, for the simplified homogeneous rain model, we found that the effect is smallest between 16 and 19 GHz, the exact frequency depending on the criterion used to measure the variation.

Using the empirical distribution of D'' ([5]), one can estimate the covariances of the brightness temperatures at various frequencies and polarizations, when the randomness is due to DSD variations

2 mm/hr	$Tb_{10.7h}$	$Tb_{19.3v}$	$Tb_{19.3h}$	$Tb_{22.2v}$	Tb_{37v}	Tb_{37h}	$Tb_{85.5v}$	$Tb_{85.5h}$
$Tb_{10.7v}$	0.99	0.77	0.85	0.10	-0.97	-0.99	-0.74	-0.74
$Tb_{10.7h}$	1.00	0.77	0.85	0.10	-0.97	-0.99	-0.74	-0.74
$Tb_{19.3v}$		1.00	0.99	0.71	-0.88	-0.78	-0.99	-0.99
$Tb_{19.3h}$			1.00	0.61	-0.94	-0.85	-0.97	-0.97
$Tb_{22.2v}$				1.00	-0.30	-0.11	-0.74	-0.74
Tb_{37v}					1.00	0.98	0.85	0.85
Tb_{37h}						1.00	0.73	0.73
$Tb_{85.5v}$							1.00	0.99
10 mm/hr	$Tb_{10.7h}$	$Tb_{19.3v}$	$Tb_{19.3h}$	$Tb_{22.2v}$	Tb_{37v}	Tb_{37h}	$Tb_{85.5v}$	$Tb_{85.5h}$
$Tb_{10.7v}$	0.99	-0.19	0.57	-0.96	-0.99	-0.99	-0.86	-0.86
$Tb_{10.7h}$	1.00	-0.19	0.56	-0.96	-0.99	-0.99	-0.86	-0.86
$Tb_{19.3v}$		1.00	0.69	0.44	0.09	0.09	-0.32	-0.32
$Tb_{19.3h}$			1.00	-0.33	-0.65	-0.64	-0.90	-0.90
$Tb_{22.2v}$				1.00	0.93	0.93	0.70	0.70
Tb_{37v}					1.00	0.99	0.91	0.91
Tb_{37h}						1.00	0.91	0.91
$Tb_{85.5v}$							1.00	0.99
20 mm/hr	$Tb_{10.7h}$	$Tb_{19.3v}$	$Tb_{19.3h}$	$Tb_{22.2v}$	Tb_{37v}	Tb_{37h}	$Tb_{85.5v}$	$Tb_{85.5h}$
$Tb_{10.7v}$	0.99	-0.91	-0.83	-0.97	-0.99	-0.99	-0.94	-0.94
$Tb_{10.7h}$	1.00	-0.91	-0.83	-0.97	-0.99	-0.99	-0.93	-0.93
$Tb_{19.3v}$		1.00	0.98	0.98	0.93	0.93	0.72	0.72
$Tb_{19.3h}$			1.00	0.93	0.85	0.85	0.59	0.59
$Tb_{22.2v}$				1.00	0.98	0.98	0.85	0.85
Tb_{37v}					1.00	0.99	0.93	0.93
Tb_{37h}						1.00	0.93	0.93
$Tb_{85.5v}$							1.00	0.99

TABLE III

Correlation coefficients as D'' is varied.

only. Again using the simplified homogeneous rain model, we calculated the covariance matrix for the nine TRMM passive microwave imager channels. Figure 2A shows the standard deviation in each channel as a function of the rain rate, while table III shows the correlation coefficients between the various channels.

Note that while the r.m.s. uncertainty at 10.7 GHz due to the variation of the mean drop size peaks at 17K (resp. 10K) for the vertical (resp. horizontal) polarization near 23 mm/hr before dropping to about 10K (resp. 7K) near 50 mm/hr, it remains rather constant and almost independent of polarization for the remaining 4 frequencies : about 3.7K at 19 and 22 GHz, 7K at 37GHz, and 5K at 85GHz. As to the correlation coefficients, after oscillating somewhat for lower rain rates, they become almost constant

above 20 mm/hr, with values as shown in the bottom third of table III. Most remarkable is the fact that they are all very close to ± 1.

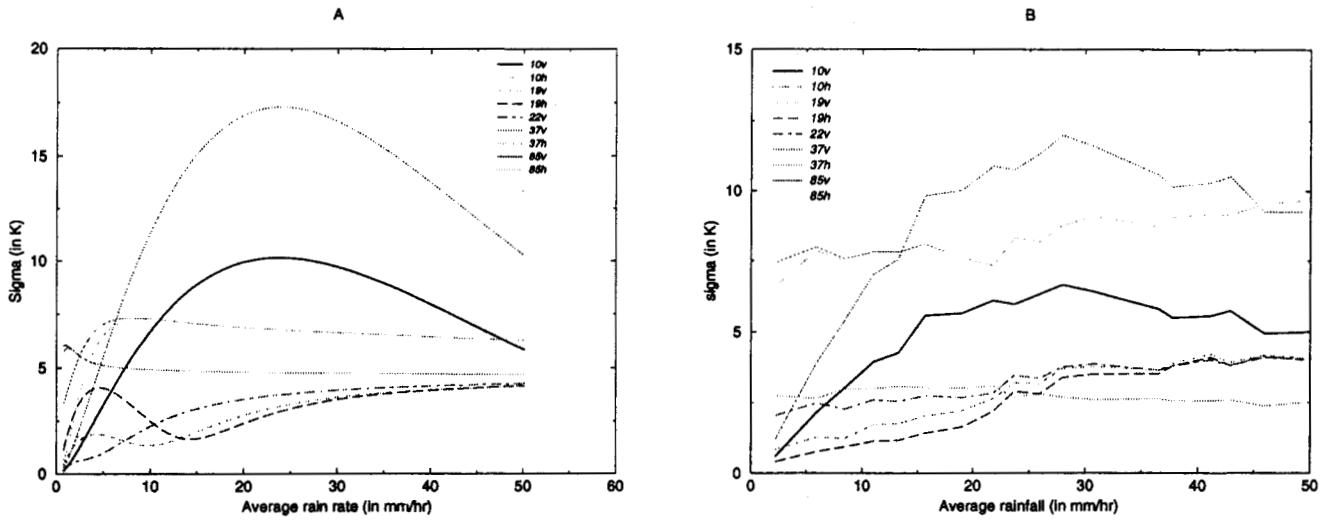

Fig. 2. *Variances of T_b as the DSD varies : model-derived standard deviations (left), and sample r.m.s. deviations from the TRMM database (right).*

These results are corroborated by the TRMM data base simulations. The subset of this database that we considered came from a hurricane simulation, which used a domain of 64x64 grid points with a resolution of 3 km. Table IV shows the correlation coefficients between the various channels, for the 10 sample rain profiles whose average rain rate was 20 mm/hr, and which can therefore be compared with the near-"steady-state" correlations at the bottom of table III. Indeed, the values are almost identical. Figure 2B shows the sample standard deviations based on the samples considered. The values at 19.3,

$\simeq$ 20 mm/hr	$Tb_{10.7h}$	$Tb_{19.3v}$	$Tb_{19.3h}$	$Tb_{22.2v}$	Tb_{37v}	Tb_{37h}	$Tb_{85.5v}$	$Tb_{85.5h}$
$Tb_{10.7v}$	0.99	-0.91	-0.84	-0.95	-0.99	-0.99	-0.84	-0.84
$Tb_{10.7h}$	1.00	-0.92	-0.85	-0.96	-0.99	-0.99	-0.82	-0.82
$Tb_{19.3v}$		1.00	0.98	0.99	0.95	0.95	0.55	0.55
$Tb_{19.3h}$			1.00	0.96	0.90	0.90	0.41	0.41
$Tb_{22.2v}$				1.00	0.98	0.98	0.65	0.65
Tb_{37v}					1.00	0.99	0.77	0.77
Tb_{37h}						1.00	0.77	0.77
$Tb_{85.5v}$							1.00	0.99

TABLE IV

Correlation coefficients for 20-mm/hr-average simulated rain events.

22.2 and 37 GHz are very close to the theoretical estimates. At 10.7 GHz they are about 30% lower, possibly due to the unavoidably small sample size. At 85 GHz they are 50% lower, undoubtedly due

to the dominant effect of scattering from ice, which is not taken into account by our simplified model.

As to the distributions MP0, MP, SS, WT and LOG, they are all more or less close approximations of the Γ distribution with average mean drop size and average relative diameter variation, as table II showed. Hence one would expect that they would produce brightness temperatures which would be accordingly close to the average. Figure 3 shows the results of the forward radiative transfer calculations for the simple homogeneous-rain model considered above. As one would expect from table II and figure

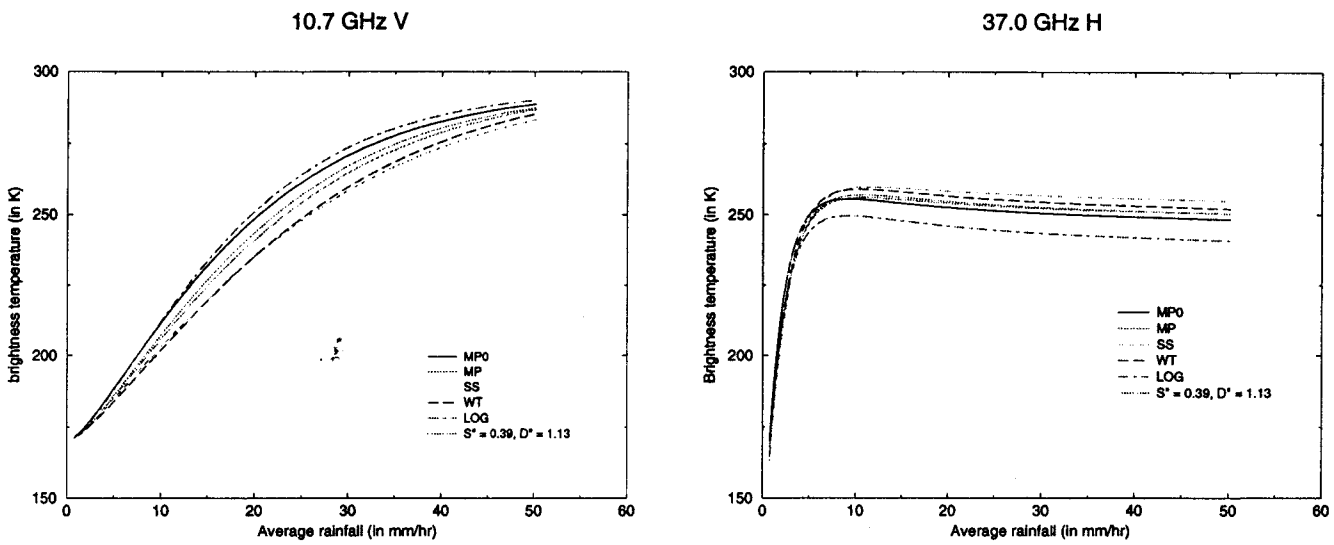

Fig. 3. *10.7GHz V-pol and 37GHz H-pol brightness temperatures for homogeneous rain with different DSDs.*

1, since LOG and MP0 have the largest mean diameters and SS the smallest, they frame the T_b vs R curves : at 10.7 GHz, for a given rain rate, LOG and MP0 produce the largest temperatures and SS the smallest; at 37 GHz, SS produces the largest temperatures and LOG and MP0 the smallest. The difference between MP0 and SS at 10.7GHz is greatest near 25 mm/hr (consistent with our covariance calculations), where it reaches 16K, or just short of one standard deviation according to our estimate. At 37 GHz, the difference between SS and MP0 at larger rain rates reaches 6K, or again just short of 1σ. Of the remaining DSDs, WT tends to behave as a smaller-than-average mean-diameter, without quite reaching the extreme of SS, while the corrected MP is closest to the curve produced with the empirical mean D'' and S'' : in fact, the difference between the MP and the mean-(D'', S'') curves is negligible.

Figures 4 and 5 show the results of the radiative transfer calculations with the TRMM cloud-model simulations. Again, MP0 and LOG produce the highest brightness temperatures at 10.7 and the lowest at 37 GHz, while SS and, to a lesser extent WT, produce low temperatures at 10.7 and high figures at 37 GHz. Figure 5 illustrates the deviation from the brightness temperatures that are produced by the

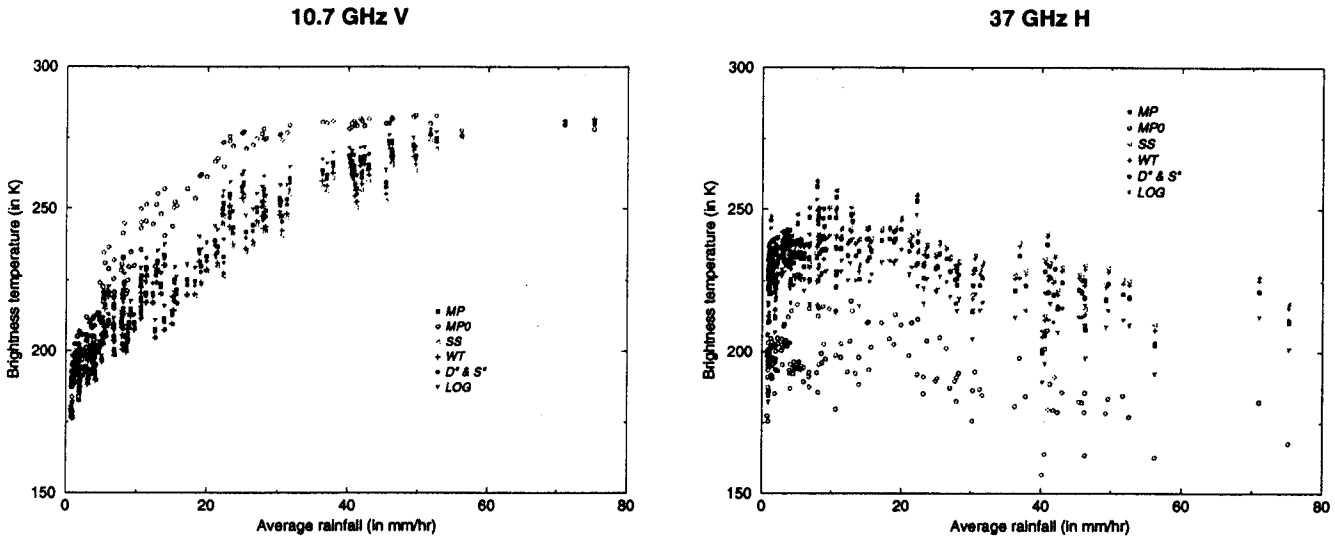

Fig. 4. *Effect of different DSDs on the brightness temperatures at 10.7 GHz V-pol and 37 GHz H-pol using cloud-model simulated events.*

mean values $D'' = 1.13$, $S'' = 0.39$, and confirms that the difference between the highest and lowest calculated temperatures reaches a maximum of about one standard deviation in all channels.

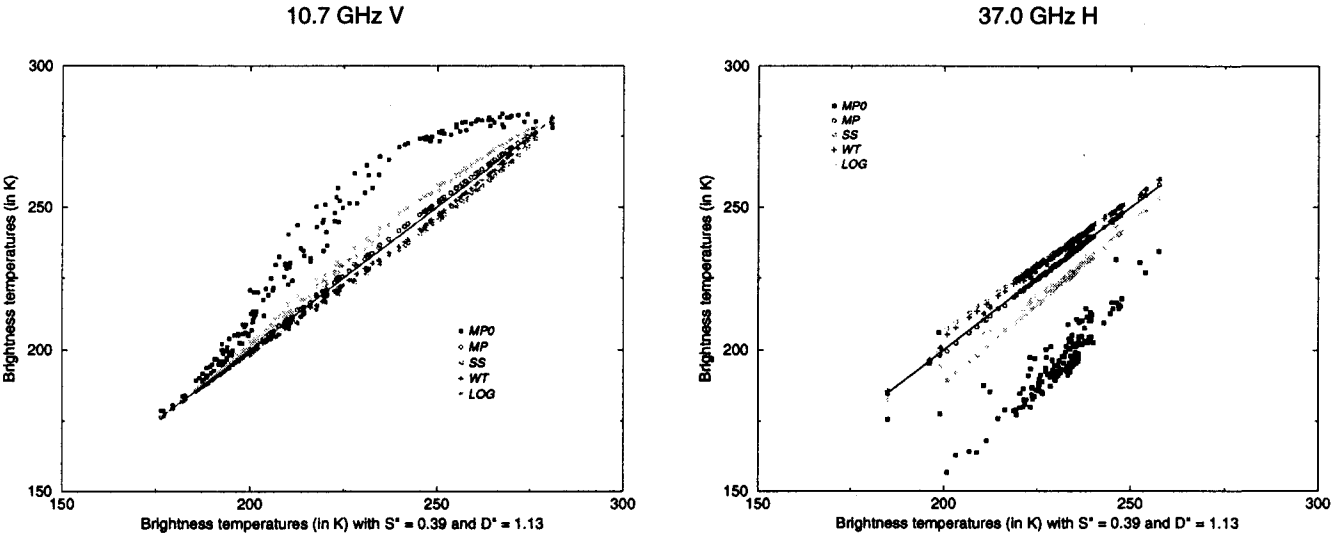

Fig. 5. *Deviation from the brightness temperatures calculated with the mean values* $D'' = 1.13$, $S'' = 0.39$.

IV. Effect on retrievals

While the conditional variances of T_b given R are interesting in themselves, one can also use them to estimate their "horizontal" counterparts and quantify the effect of the DSD on the estimated average rain rate, given a set of observed brightness temperatures. Indeed, while the vertical separation between

the curves in figures 3 and 4 is not great, a given brightness temperature would seem to correspond to widely separated rain rates. While this seems to imply a large uncertainty in the retrieval process, the actual uncertainty is reduced by the correlation between the variations in the different channels. One would also expect a bias, smaller-diameter DSDs tending to associate a given brightness temperature to higher rain rates than higher-diameter DSDs. To obtain quantitative estimates of the expected bias in the retrieved rain rates, Bayes's rule can be applied to compute the mean $\mathcal{E}\{R|T_b\}$ of the rain rate R given a set of brightness temperatures T_b, giving

$$\mathcal{E}\{R|T_b\} = \frac{\int R'\, p(T_b|R')\, p_o(R')\, dR'}{\int p(T_b|R')\, p_o(R')\, dR'} \tag{9}$$

where the conditional density $p(T_b|R')$ can be assumed approximately Gaussian to first order, and hence is determined by its mean and covariance as computed in section II. For the a priori distribution $p_o(R')$ we used a climatological log-normal density $p_o(R') = exp(-0.5(\log(R'/r_o)/\sigma_o)^2)/(R'\sigma_o\sqrt{2\pi})$, with parameters $r_o = 3$ mm/hr and $\sigma_o = 1$ as computed from the GATE data ([15]). Various other reasonable expressions for p_o were also tested, including a uniform density between 0 and 100 mm/hr, with negligible effect on the resulting mean. Figure 6 shows the biases which would result from using the

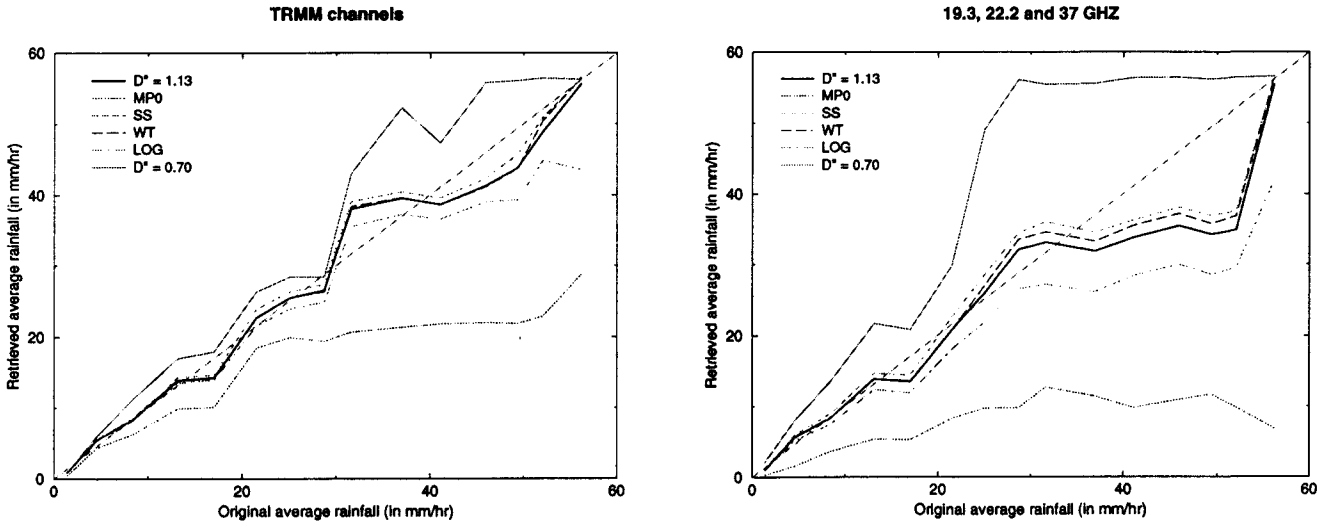

Fig. 6. *Expected biases of the various DSDs, with and without the 10.7GHz channel.*

various DSDs discussed above. The corrected MP is not shown because it overlays the case $D'' = 1.13$ almost exactly. As expected, the smaller-than-average mean-diameter DSDs such as SS and WT (and the uncorrelated-parameters Γ with $D'' = 0.7$) on the whole show positive biases, while the larger-than-average mean-diameter DSDs such as LOG and MP0 show negative biases, reaching an impressive -50% in the case of the uncorrected MP0. These biases grow if one ignores the 10.7GHz channel, although in practice the effect on one's retrievals will depend crucially on the resolution of the various channels,

as well as on other sources of error which this study did not take into account.

V. Conclusions

Variations in the DSD have a significant effect on radiative transfer calculations of the associated microwave brightness temperatures. In the case of a 50 degree look angle, and for rain over a 290K ocean surface, the effect depends on frequency and average rain rate. At 10.7 GHz, the standard deviation due to DSD variability reaches 17K at vertical polarization (10K at horizontal) when the rain rate averages 23 mm/hr, before dropping to about 10K (resp. 7K) at higher rain rates. At 37 GHz, it remains near 7K. The effect is smallest between 16 and 19 GHz, where the standard deviation drops to 3.7K. At 85 ice scattering dominates; even if it didn't, the DSD-generated uncertainty would be a low 5K. In general, smaller-mean-diameter DSDs (such as that of Sekhon-Srivastava ([12]) and to a lesser extent that of Willis-Tattleman ([16])) produce lower brightness temperatures below 16 GHz, higher ones above 19 GHz, whereas larger-mean-diameter DSDs (such as the unmodified Marshall-Palmer ([9]) and the logarithmic Feingold-Levin ([9])) produce higher brightness temperatures below 16 GHz, lower ones above 19 GHz. The covariance matrix between the various TRMM passive microwave channels due to DSD variability changes with the average rain rate but the correlation coefficients reach "steady state" above 20 mm/hr : the correlation coefficients between the 10.7 GHz channels and the higher-frequency ones approach -1, while all other correlation coefficients approach +1. The individual variances are given in figure 2. The effect on rain retrievals is more significant in the case of larger-mean-diameter DSDs than the forward variances would suggest. Not only do these DSDs generally tend to associate lower average rain rates to a given set of brightness temperatures, in the case of the unmodified Marshall-Palmer DSD, one can expect the bias to reach -50%. Finally, while the lowest channel considered, 10.7 GHz, is quite sensitive to DSD variations, it can also be quite important in reducing the bias in passive-microwave rain retrievals.

VI. Acknowledgements

We wish to thank Chris Kummerow for providing his Eddington radiative transfer model. We also thank Eric Smith and Peter Bauer for many helpful discussions. This work was performed at the Jet Propulsion Laboratory, California Institute of Technology, under contract with the National Aeronautics and Space Administration.

REFERENCES

[1] G. Feingold and Z. Levin, "The lognormal fit of raindrop spectra from frontal convective clouds in Isreal", *J. Climate Appl. Meteor.*, vol. 25, pp 1346-1363, 1986.

[2] E.E. Gossard, R.G. Strauch, D.C. Welsh, and S.Y. Matrosov, "Cloud layer, Particle Identification, and Rain-Rate Profiles from ZRV_f Measurements by Clean-Air Doppler Radars", *J. Atmos. Oceanic Technol.*, vol. 9, pp 108-119, 1992.

[3] R. Gunn and G.D. Kinzer, "The terminal velocity of fall for water droplets in stagnant air", *J. Meteorol.*, vol. 6, pp 243-248, 1949.

[4] Z.S. Haddad, S.L. Durden, and E. Im, "Parametrizing the raindrop size distribution", *J. Appl. Meteor.*, vol. 35, no. 1, pp 3-13, January, 1996.

[5] Z.S. Haddad, D.A. Short, S.L. Durden, E. Im, S. Hensley, M.B. Grable and R. A. Black, "A new parametrization of the rain drop size distribution", , *IEEE Tran. geosc. remote sensing*, vol. 35. no. 3, pp 532-539, May, 1997.

[6] J. Joss and E.G. Gori, "Shapes of raindrop size distributions", *J. Appl. Meteor.*, vol. 17, pp 1054-1061, 1978.

[7] C. Kummerow, W.S. Olson and L. Giglio, "A simplified scheme for obtaining precipitation and vertical hydrometeor profiles from passive microwave sensors", *IEEE Trans. Geosci.*, vol. 34, no. 5, pp 1213-1232, 1996.

[8] C. Kummerow, "On the accuracy of the Eddington approximation for radiative-transfer in the microwave frequencies", *J. Geo. Res. A*, vol. 98, pp 2757-2765, 1993.

[9] J. S. Marshall and W. M. Palmer, "Relation of raindrop size to intensity", *J. Meteor.*, vol. 5, pp 165-166, 1948.

[10] A. Mugnai, E.A. Smith and G.J. Tripoli, "Foundations for statistical-physical precipitation retrieval from passive microwave frequencies. Part II : Emission-source and generalized eighting-function properties of a time-dependent cloud radiation model", *J. Appl. Meteor.*, vol. 32, pp 17-39, 1993.

[11] R. S. Sekhon and R. C. Srivastava, "Snow size spectra and radar reflectivity", *Jour. Atmos. sciences*, Vol. 27, pp 299-307, March 1970.

[12] R. S. Sekhon and R. C. Srivastava, "Doppler radar obeservations of drop size distributions in a thunderstorm", *Jour. Atmos. sciences*, pp 983-994, September 1971.

[13] E.A. Smith, A. Mugnai, H.J. Copper, G.J. Tripoli and X. Xiang, "Foundations for statistical-physical precipitation retrieval from passive microwave frequencies. Part I : Brightness-

temperature properties of a time-dependent cloud radiation model", *J. Appl. Meteor.*, vol. 31, pp 506-531, 1992.

[14] A. Waldvogel, "The N_0 jump of raindrop spectra", *J. Atmos. sciences*, vol. 31, pp 1648-1661, 1974.

[15] T.T. Wilheit, "Error analysis for the tropical rainfall measuring mission", in *Tropical Rainfall Measurements*, J.S. Theon and N. Fugono, eds., A. Deepak publishing, pp 377-385, 1988.

[16] P. T. Willis and P. Tattelman, "Drop-size distributions associated with intense rainfall", *J. Appl. Meteor.*, vol. 28, pp 3-15, 1989.

10.7 GHz V

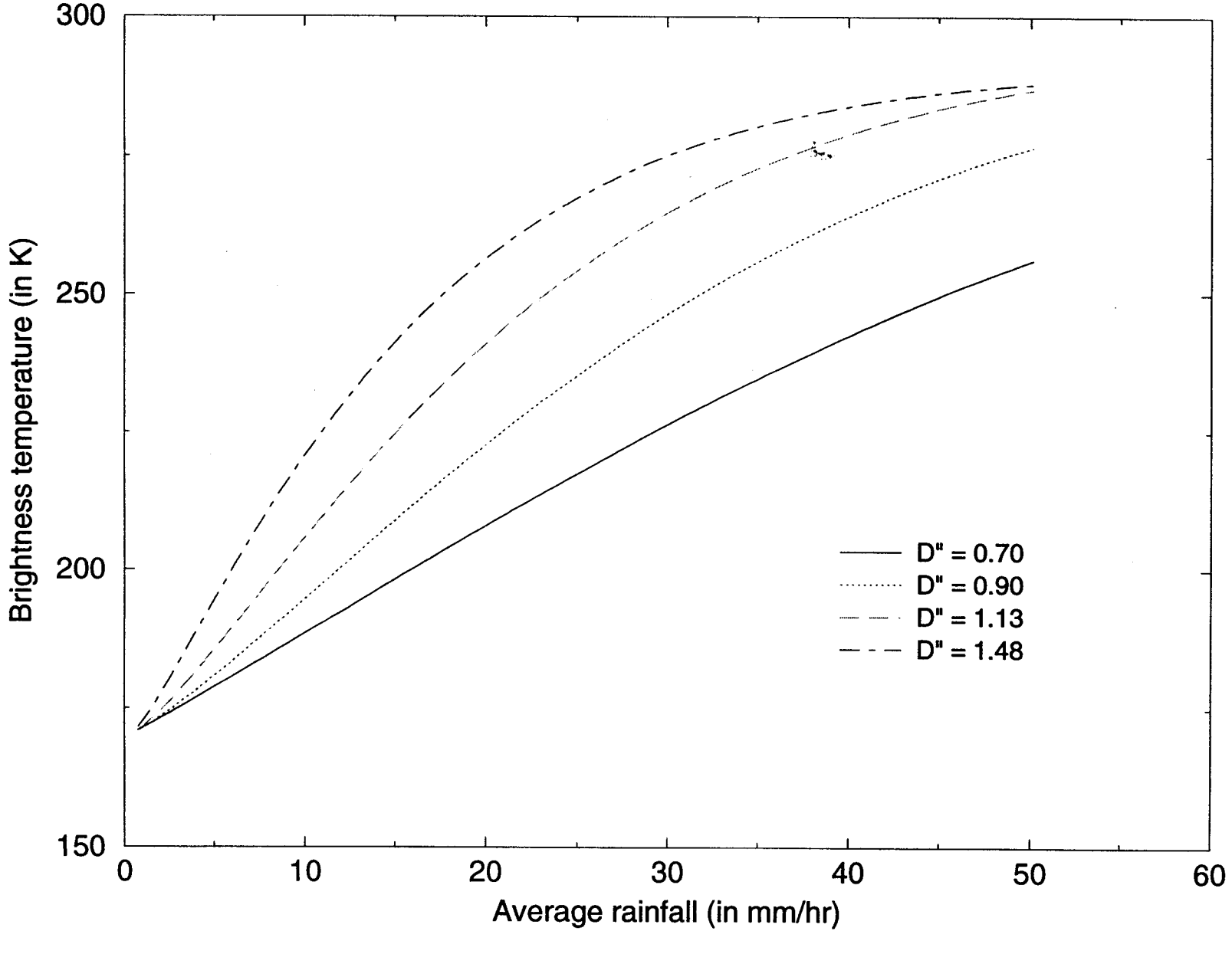
300
250
200
150
Brightness temperature (in K)
0
10
20
30
40
50
60
Average rainfall (in mm/hr)
D" = 0.70
D" = 0.90
D" = 1.13
D" = 1.48

37.0 GHz H

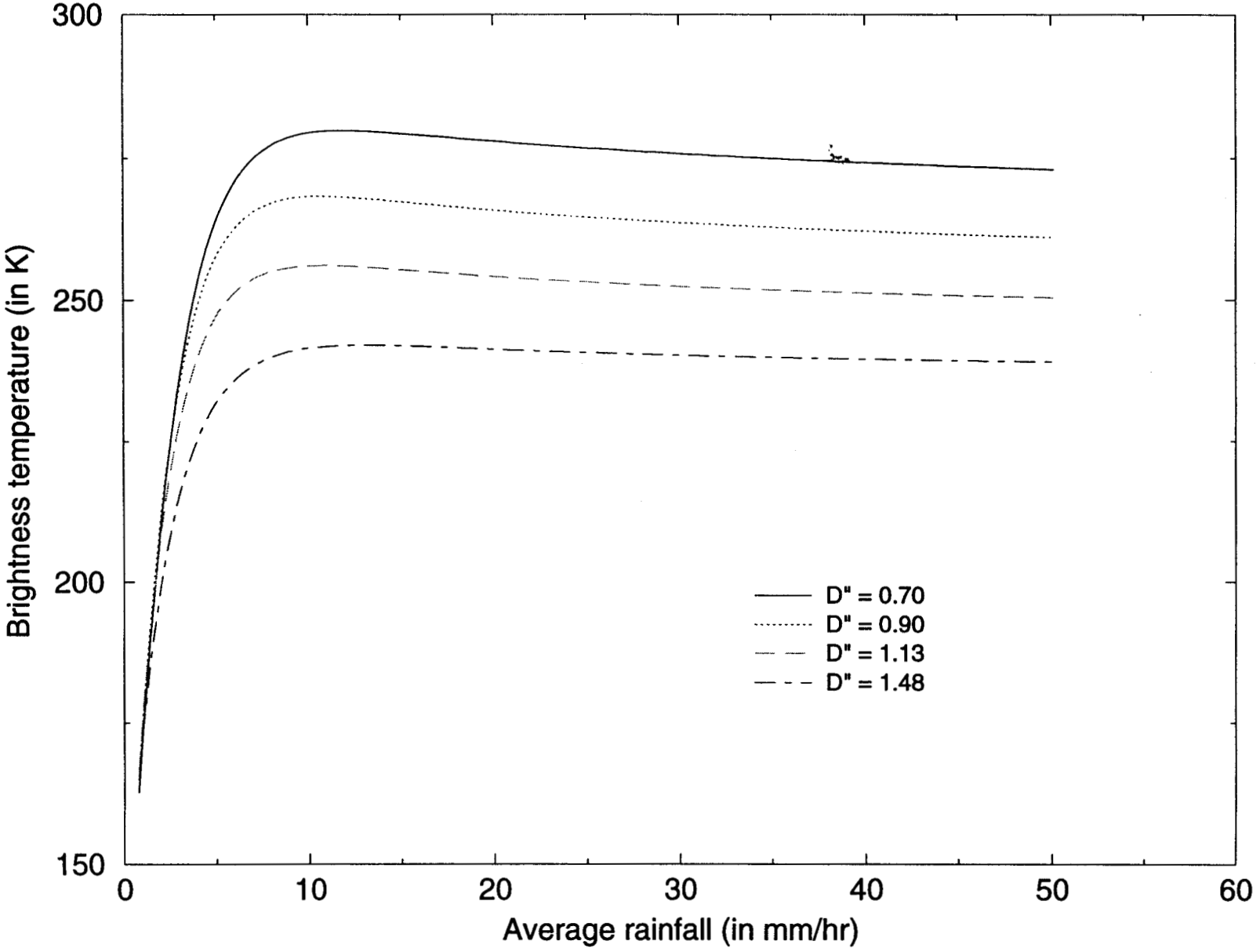
300
250
200
150
0
10
20
30
40
50
60
Brightness temperature (in K)
Average rainfall (in mm/hr)
D" = 0.70
D" = 0.90
D" = 1.13
D" = 1.48

A

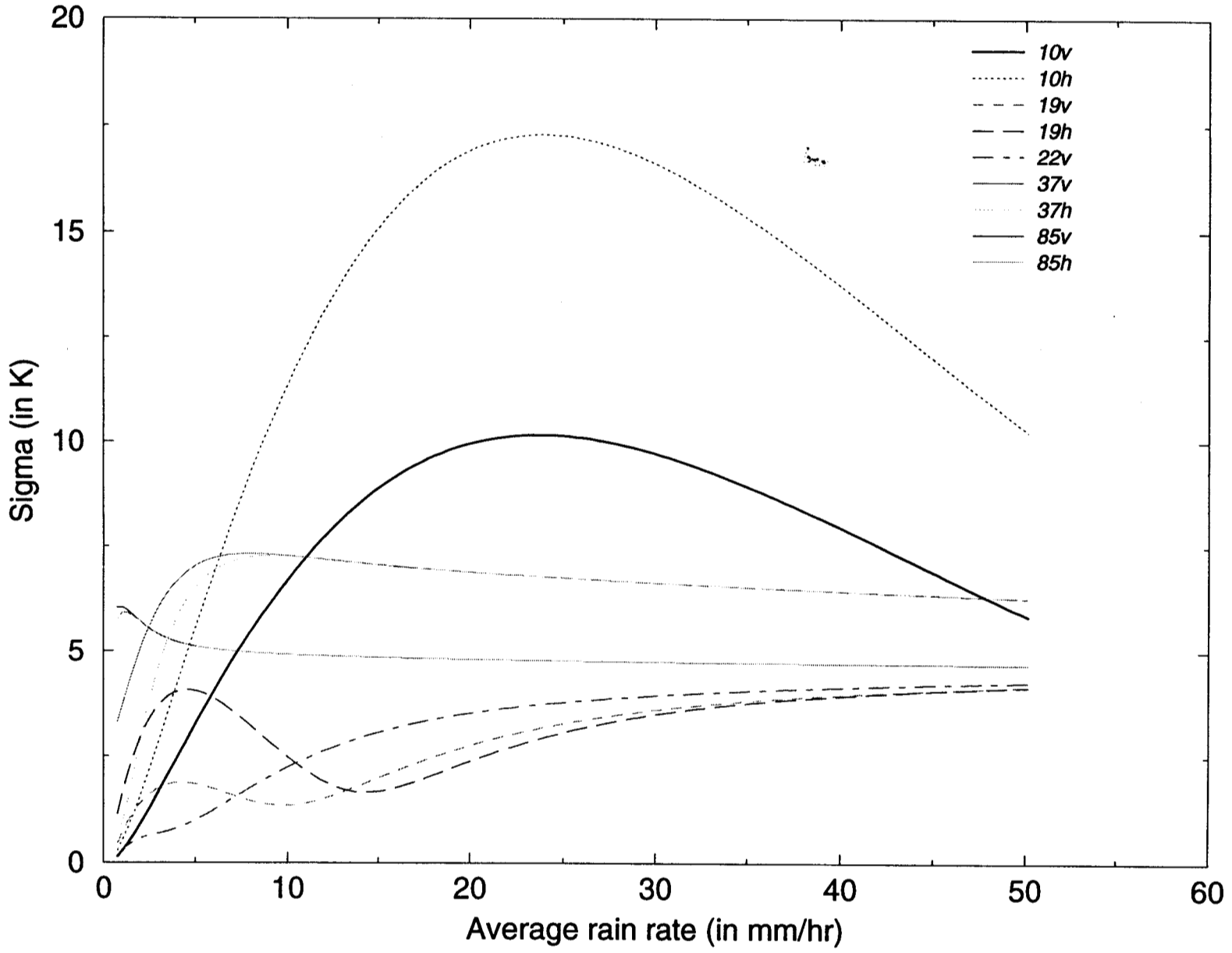
20
15
10
5
0
0
10
20
30
40
50
60
Sigma (in K)
Average rain rate (in mm/hr)
10v
10h
19v
19h
22v
37v
37h
85v
85h

B

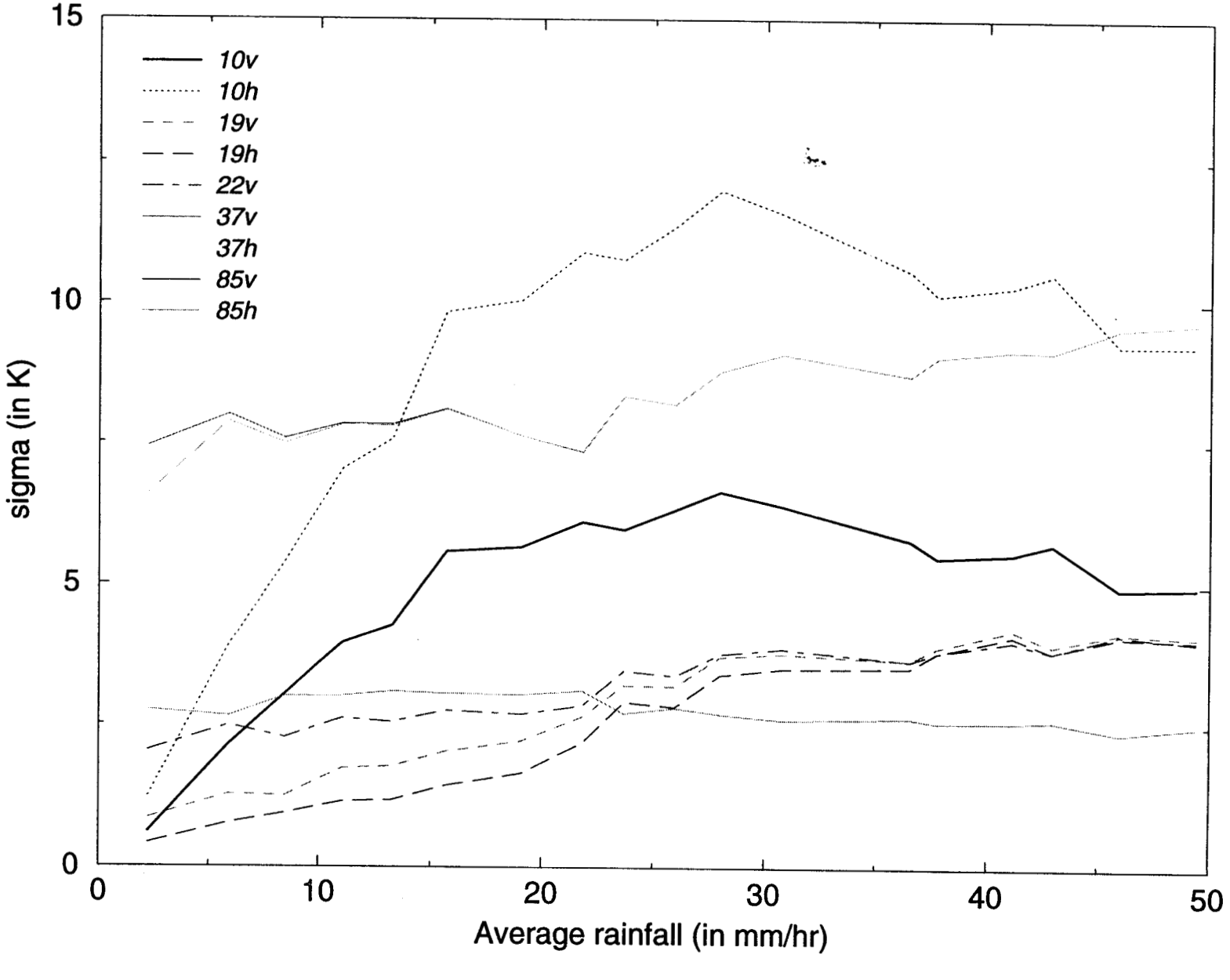
15
10
5
0
0
10
20
30
40
50
sigma (in K)
Average rainfall (in mm/hr)
10v
10h
19v
19h
22v
37v
37h
85v
85h

10.7 GHz V

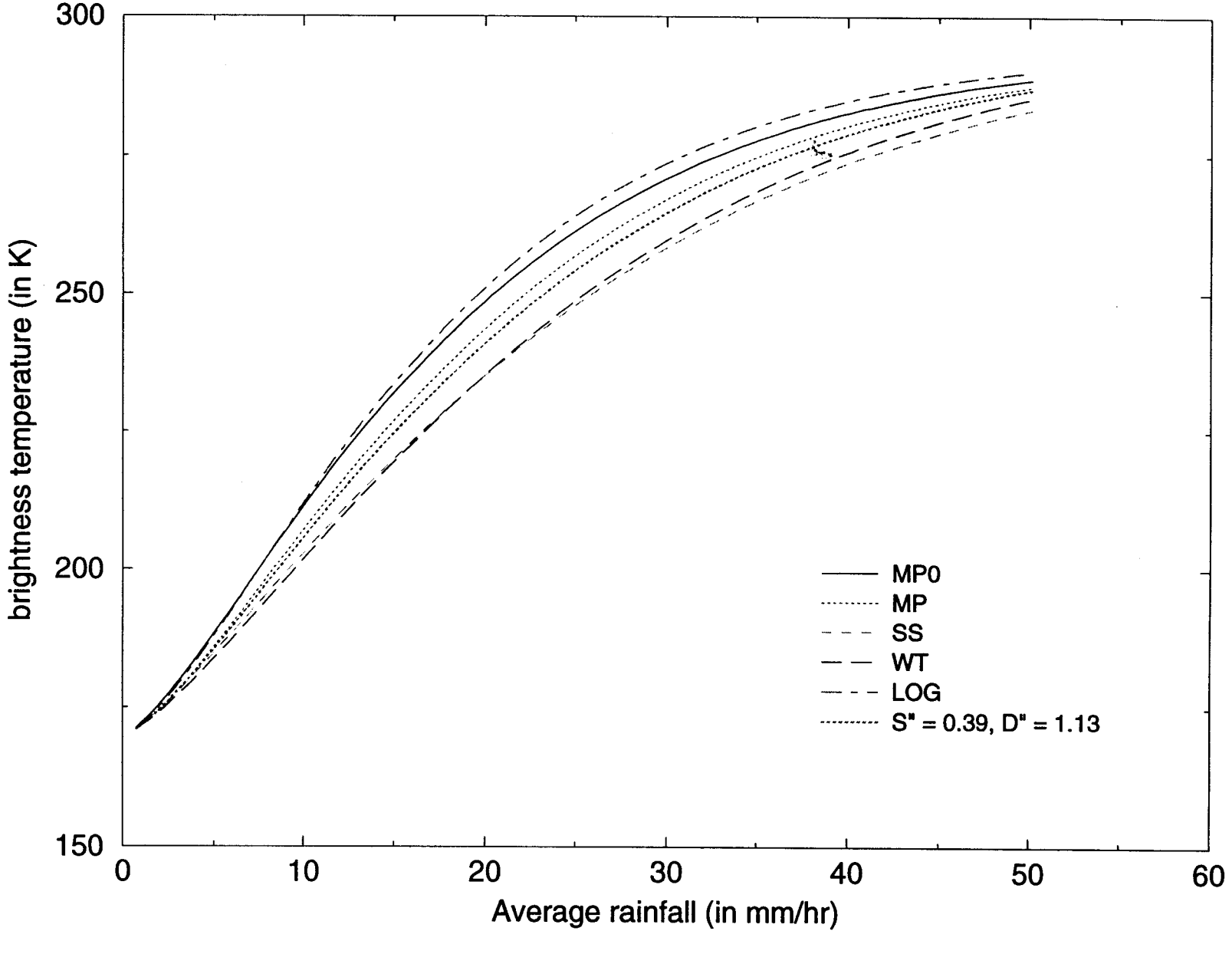
300
250
200
150
brightness temperature (in K)
0
10
20
30
40
50
60
Average rainfall (in mm/hr)
MP0
MP
SS
WT
LOG
S" = 0.39, D" = 1.13

37.0 GHz H

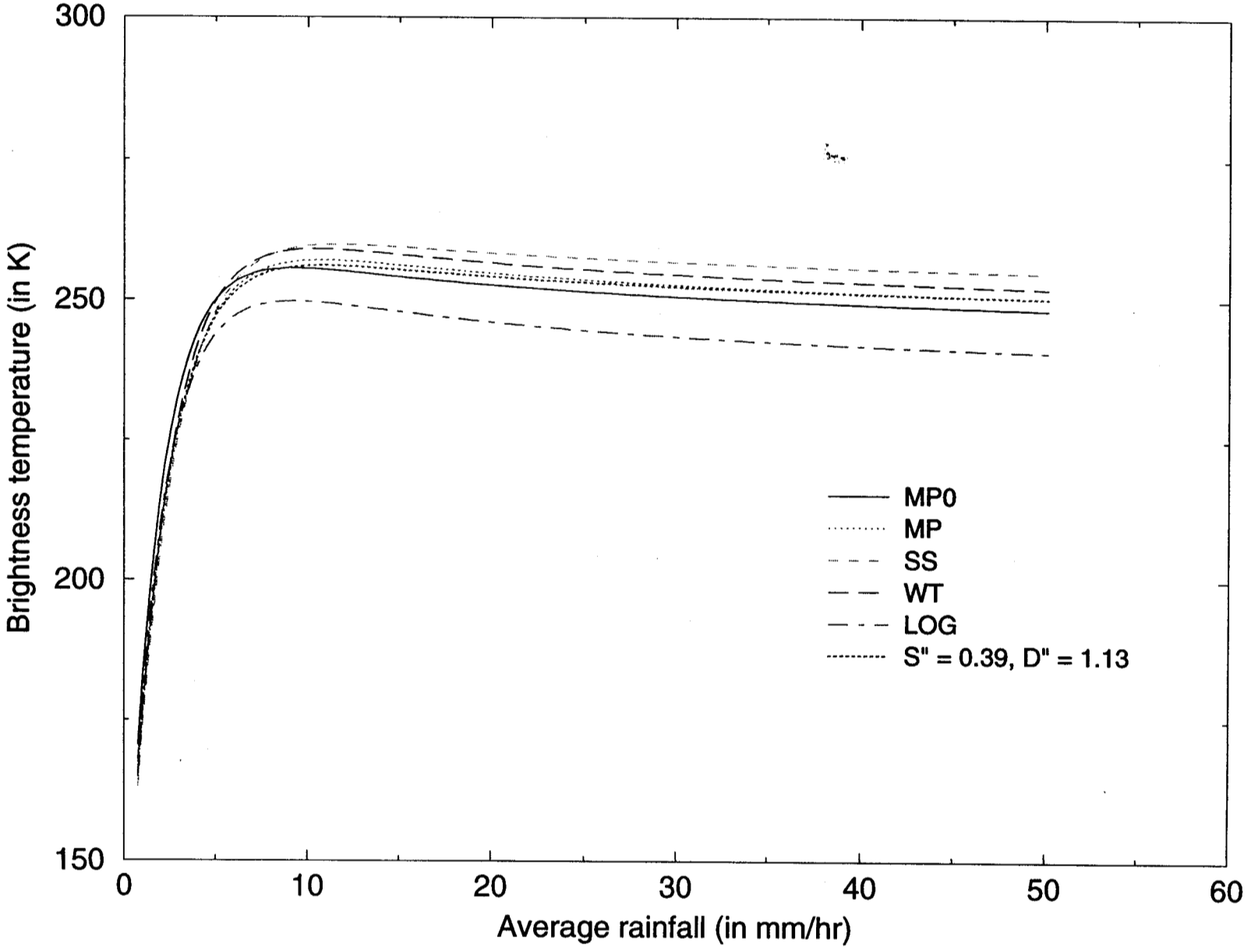
300
250
200
150
0
10
20
30
40
50
60
Brightness temperature (in K)
Average rainfall (in mm/hr)
MP0
MP
SS
WT
LOG
S" = 0.39, D" = 1.13

10.7 GHz V

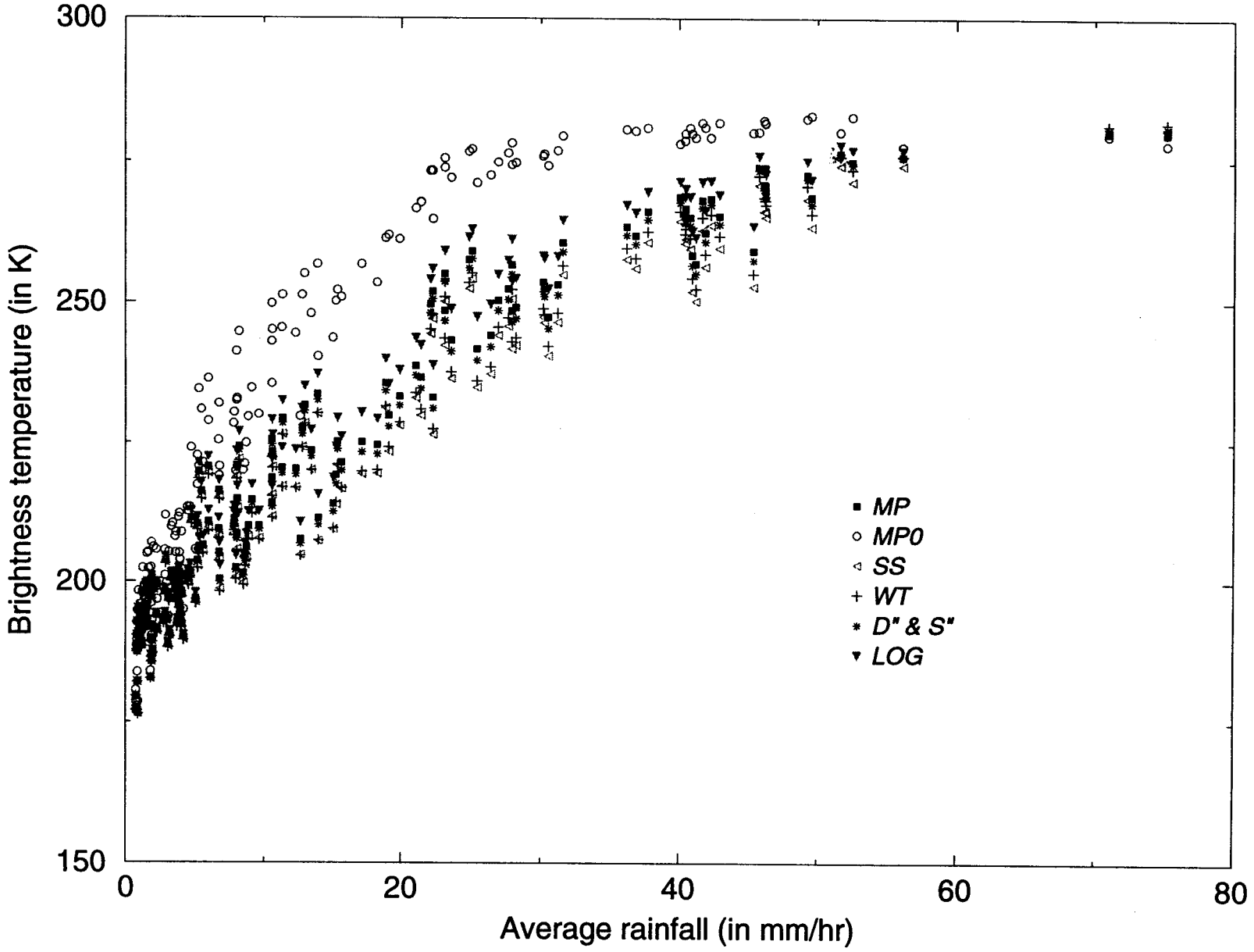
300
250
200
150
0
20
40
60
80
Brightness temperature (in K)
Average rainfall (in mm/hr)
MP
MP0
SS
WT
D" & S"
LOG

37 GHz H

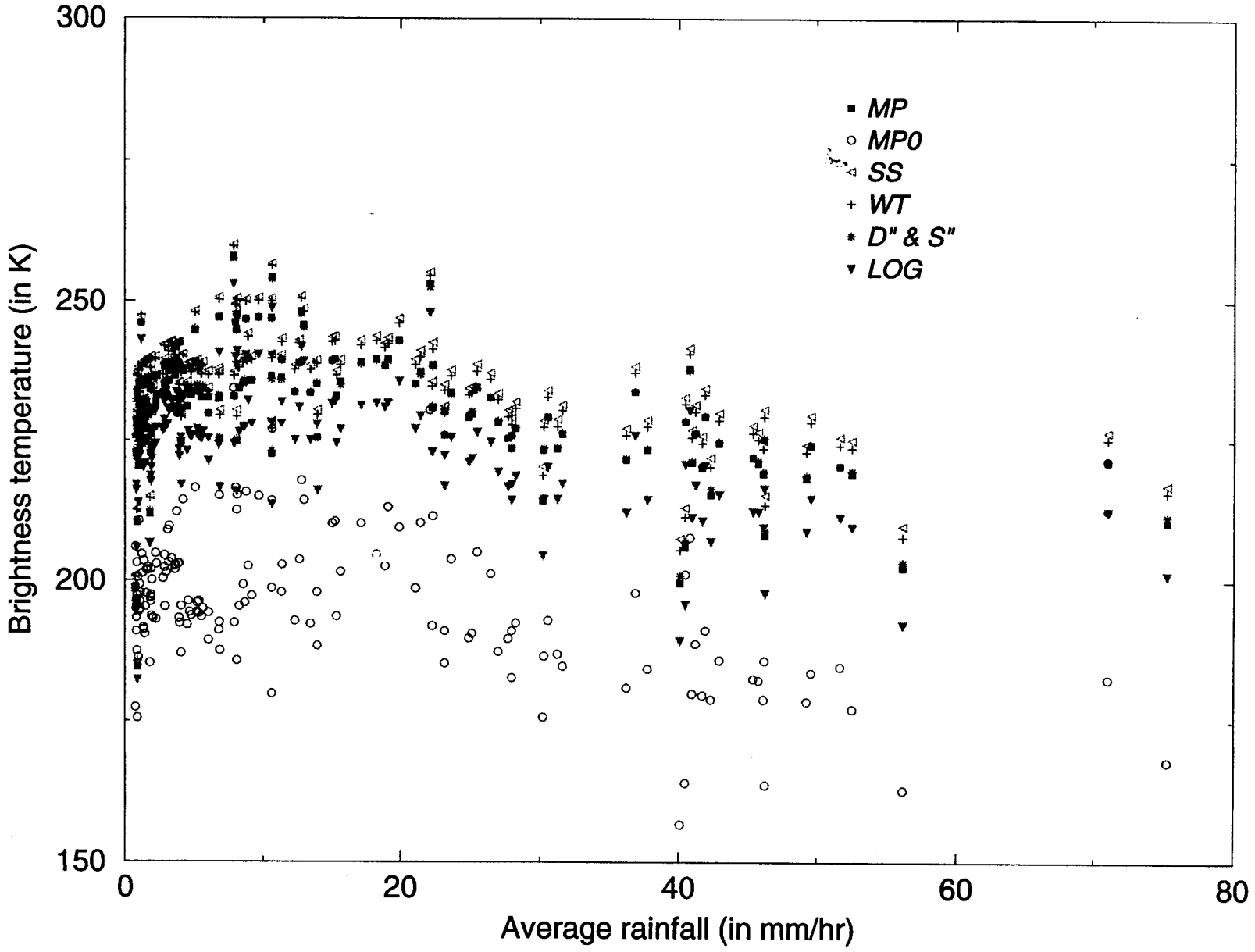
300
250
200
150
0
20
40
60
80
Brightness temperature (in K)
Average rainfall (in mm/hr)
MP
MP0
SS
WT
D" & S"
LOG

10.7 GHz V

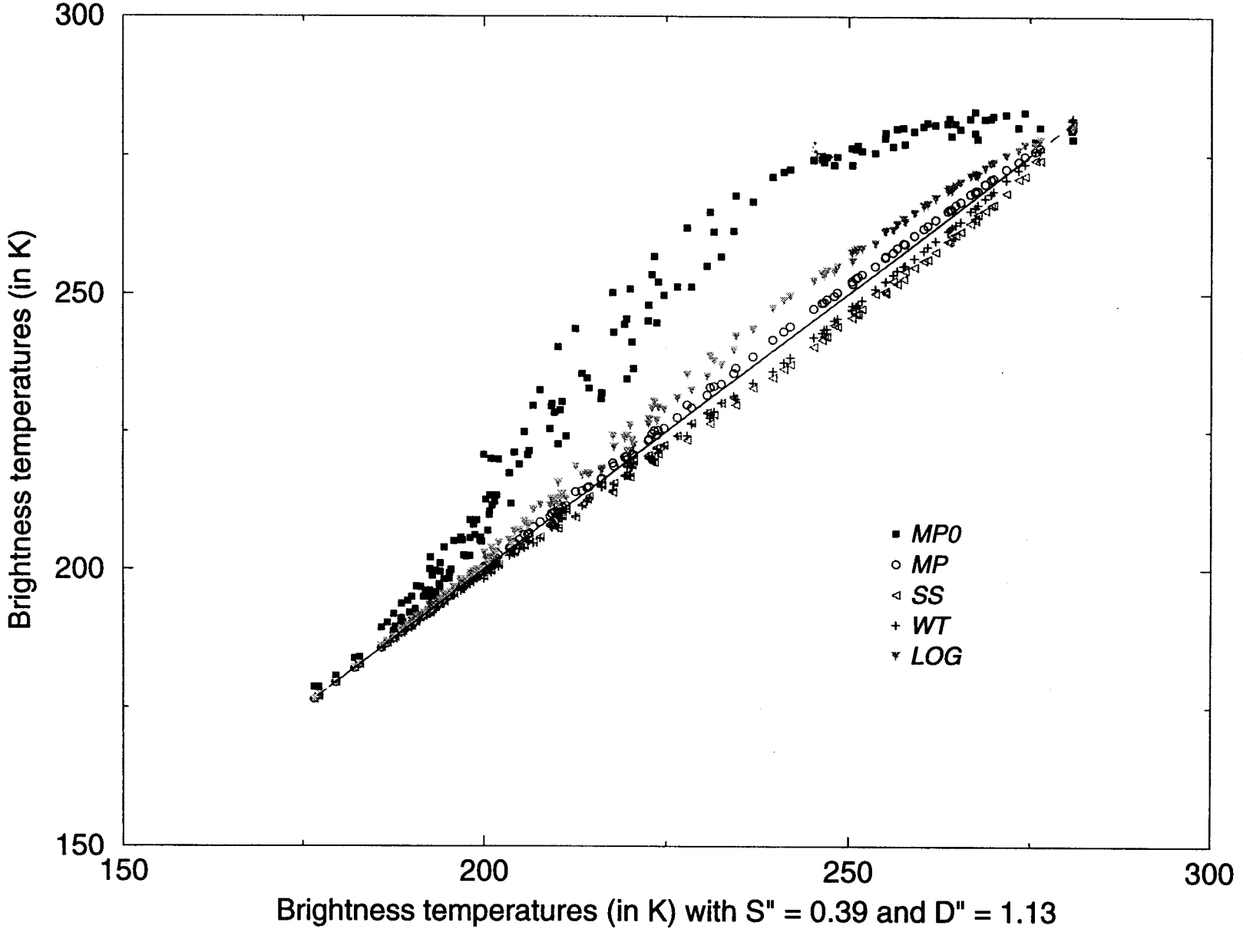
300
250
200
150
150
200
250
300
Brightness temperatures (in K)
Brightness temperatures (in K) with S" = 0.39 and D" = 1.13
MP0
MP
SS
WT
LOG

37.0 GHz H

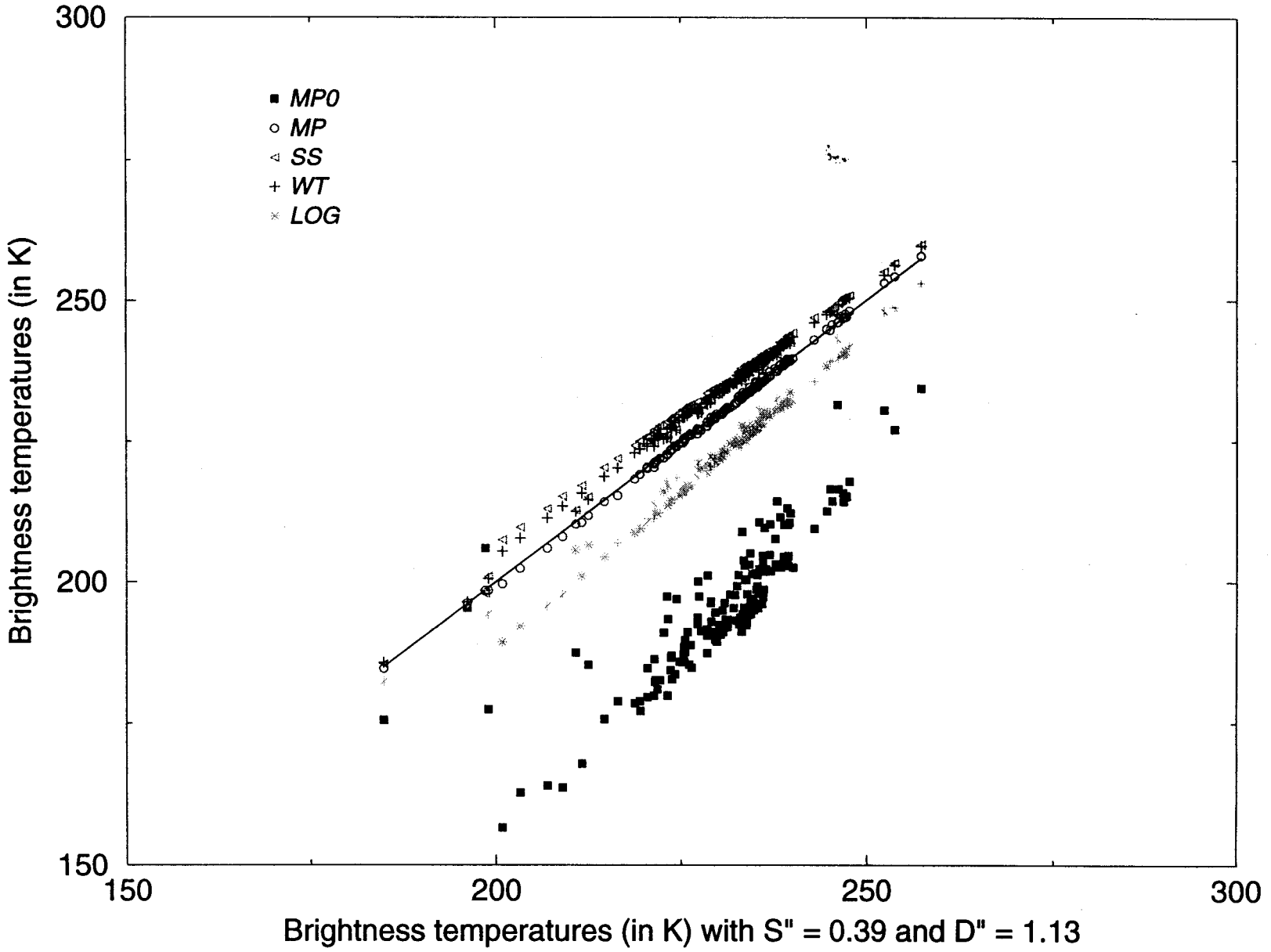
MP0
MP
SS
WT
LOG
300
250
200
150
150
200
250
300
Brightness temperatures (in K)
Brightness temperatures (in K) with S" = 0.39 and D" = 1.13

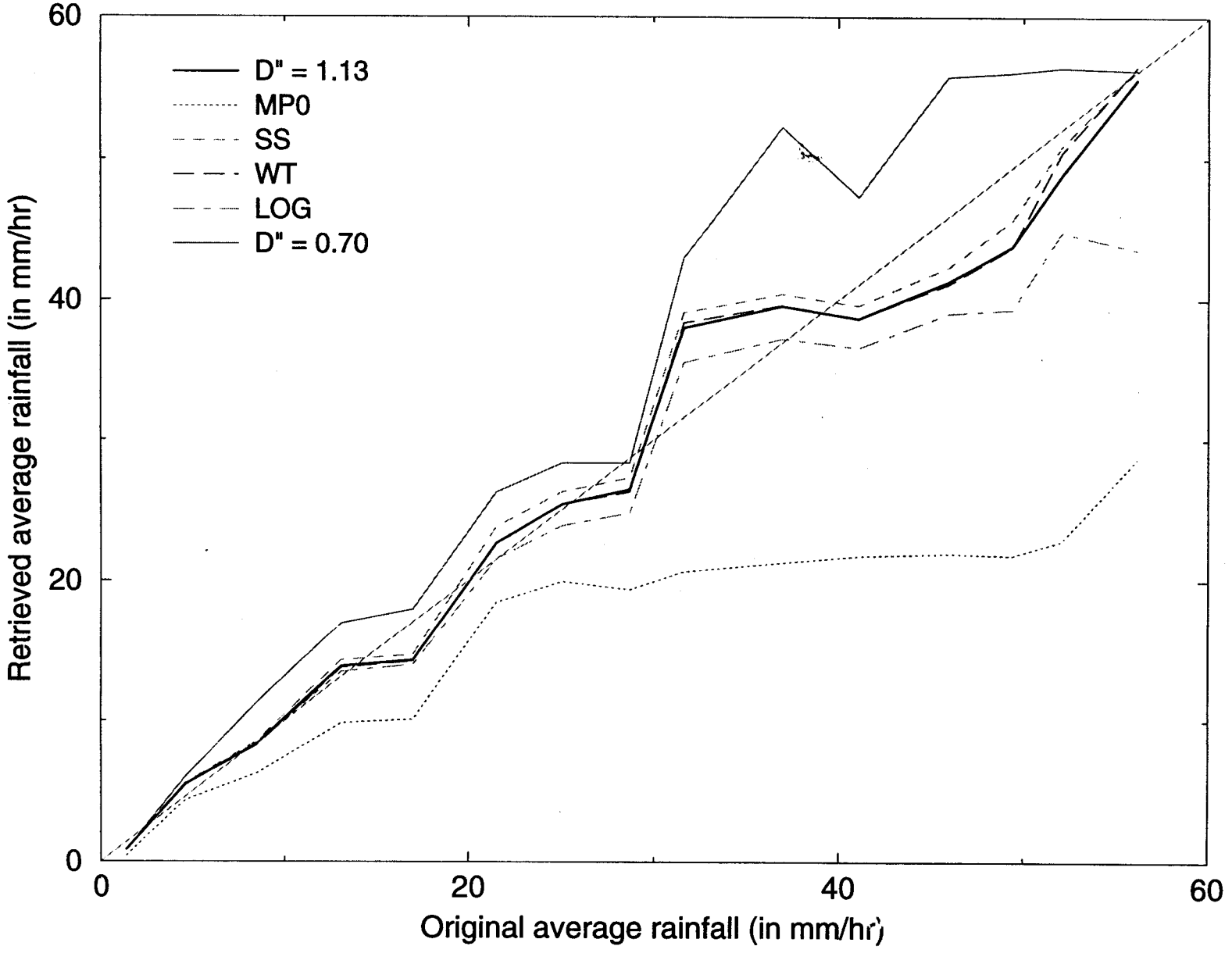
TRMM channels
D" = 1.13
MP0
SS
WT
LOG
D" = 0.70
Retrieved average rainfall (in mm/hr)
Original average rainfall (in mm/hr)
0
20
40
60

19.3, 22.2 and 37 GHZ